

# Agarose-Based Microfluidic Device for Point-of-Care Concentration and Detection of Pathogen

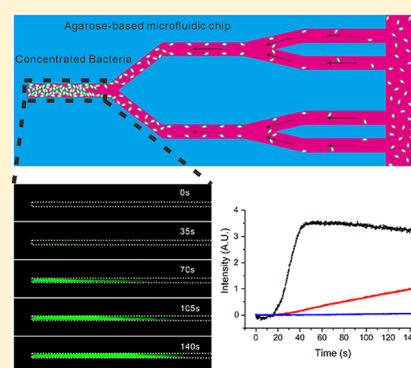
Yiwei Li,<sup>†,§</sup> Xinghua Yan,<sup>†,§</sup> Xiaojun Feng,<sup>§</sup> Jie Wang,<sup>§</sup> Wei Du,<sup>§</sup> Yachao Wang,<sup>§</sup> Peng Chen,<sup>§</sup> Liang Xiong,<sup>‡</sup> and Bi-Feng Liu<sup>\*§</sup>

<sup>§</sup>Britton Chance Center for Biomedical Photonics at Wuhan National Laboratory for Optoelectronics – Hubei Bioinformatics & Molecular Imaging Key Laboratory, Systems Biology Theme, Department of Biomedical Engineering, College of Life Science and Technology, Huazhong University of Science and Technology, Wuhan, Hubei 430074, China

<sup>‡</sup>Liyuan Hospital, Tongji Medical College, Huazhong University of Science and Technology, Wuhan, Hubei 430074, China

## S Supporting Information

**ABSTRACT:** Preconcentration of pathogens from patient samples represents a great challenge in point-of-care (POC) diagnostics. Here, a low-cost, rapid, and portable agarose-based microfluidic device was developed to concentrate biological fluid from micro- to picoliter volume. The microfluidic concentrator consisted of a glass slide simply covered by an agarose layer with a binary tree-shaped microchannel, in which pathogens could be concentrated at the end of the microchannel due to the capillary effect and the strong water permeability of the agarose gel. The fluorescent *Escherichia coli* strain OP50 was used to demonstrate the capacity of the agarose-based device. Results showed that 90% recovery efficiency could be achieved with a million-fold volume reduction from 400  $\mu\text{L}$  to 400 pL. For concentration of  $1 \times 10^3$  cells  $\text{mL}^{-1}$  bacteria, approximately ten million-fold enrichment in cell density was realized with volume reduction from 100  $\mu\text{L}$  to 1.6 pL. Urine and blood plasma samples were further tested to validate the developed method. In conjunction with fluorescence immunoassay, we successfully applied the method to the concentration and detection of infectious *Staphylococcus aureus* in clinics. The agarose-based microfluidic concentrator provided an efficient approach for POC detection of pathogens.



Developments in microfluidics have significantly improved the way we perform high-throughput and low-cost diagnoses of infectious diseases.<sup>1</sup> A diagnosis system should not only detect pathogens sensitively and accurately but also include a novel module for sample preparation, which significantly reduces the time required and improves the throughput.<sup>2</sup> Traditional processes of sample pretreatment, preconcentration, and prolonged culture of the potential pathogen often require hours or even days to complete.<sup>3,4</sup> Rapid sample preparation and preconcentration of potential pathogens from patient samples such as spinal fluid, blood, and saliva are urgently needed in point-of-care (POC) infectious disease diagnostics, especially for some uncultured bacteria.<sup>5</sup>

Sample preparation involves the purification and preconcentration of infectious bacteria. Traditionally, concentration is performed in the laboratory using commercial equipment such as a centrifuge. However, the use of traditional equipment has three disadvantages for POC testing. First, the centrifuge used is not portable. Second, as the volume of sample grows smaller, prevention of contamination becomes difficult. Finally, concentration of bacteria in a microliter or even nanoliter sample is still a challenge. In comparison to traditional laboratory methods, microfluidic methods for bacteria concentration are much more rapid, portable, sample-saving, and

labor-saving.<sup>6,7</sup> Highly integrated microfluidic devices also avoid sample contamination.

Existing microfluidic approaches for bacteria concentration include immunological, electrodynamic, microfilter, and various other methods. Some researchers have combined immunomagnetic particle methods with microfluidics for pathogen isolation and detection, which provides a simple strategy for effective and inexpensive disease detection.<sup>8,9</sup>

Several studies have previously succeeded in cell concentration using electrodynamic methods.<sup>10–21</sup> Since the bacterial surfaces are negatively charged, manipulating cells to move in microchannels is easy when exposed to an electric field. However, electrodynamic methods require specific equipment, including additional electrodes and accurate power supplies. Such systems are not only expensive but also nonportable, which is not suitable for the POC detection of infectious bacterial diseases. Since the electrodynamic approach is dependent on the surface charge of the infectious bacteria, it is not suitable for all kinds of pathogens. Additionally, the heterogeneity of individual cells also makes this method uncontrollable.

Received: July 8, 2014

Accepted: September 29, 2014

Published: September 29, 2014

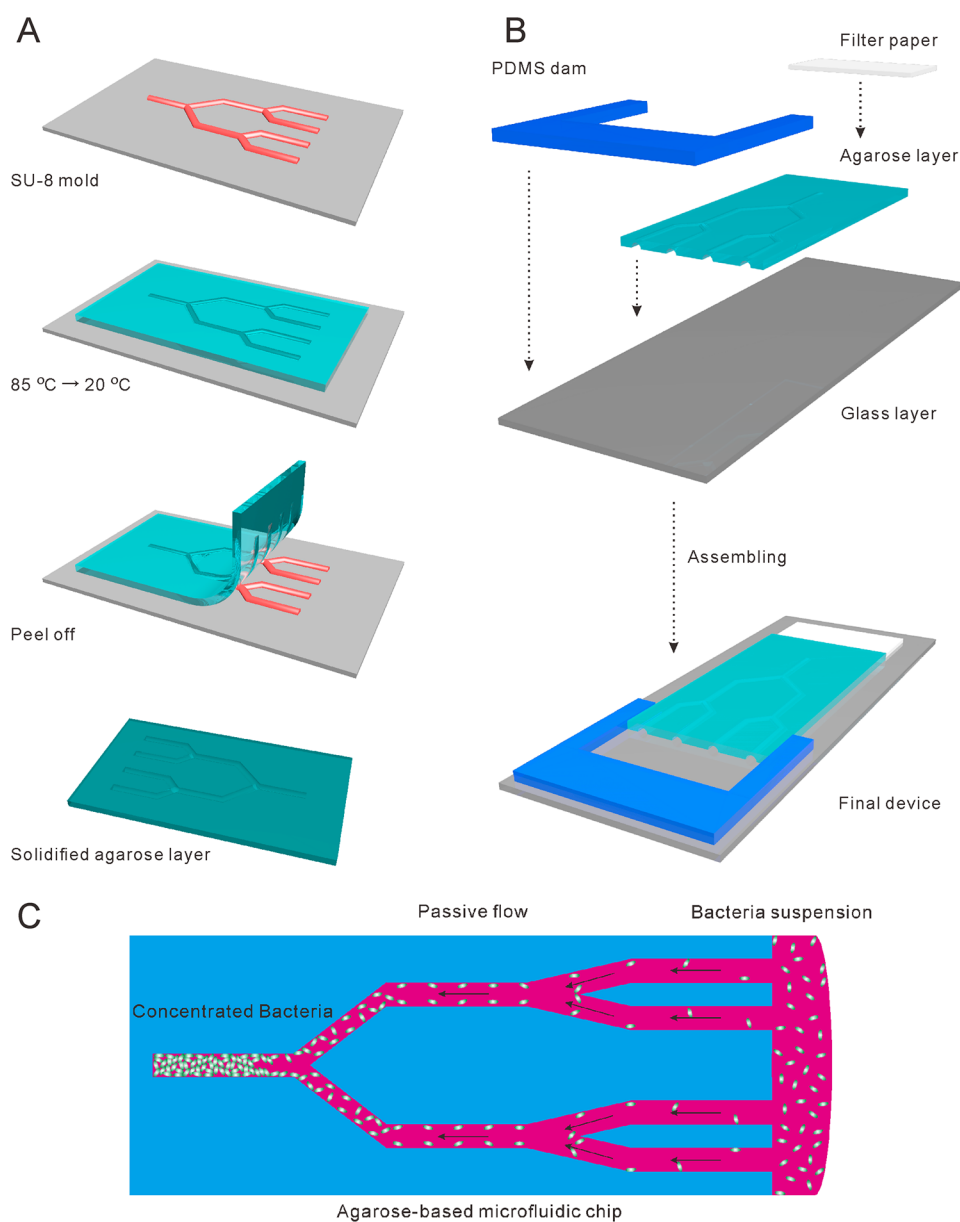


**Figure 1.** (A) Schematic of agarose microchip fabrication. (B) Assembly of final agarose-based microfluidic device. (C) Schematic of the passive bacteria concentration process.

Microfilters have been used to trap and collect microbes fabricated inside microfluidic channels.<sup>22–27</sup> This method requires the pore size of the porous monolith to be smaller than the size of the infectious bacteria. During the enrichment procedure, the solution passed through, while the bacteria were trapped and enriched in the microchannel. A filter-based immunofluorescence labeling microfluidic system was developed by Liu's group for the rapid detection of microbial cells.<sup>27</sup> Lay et al. designed a microfilter featuring a raindrop bypass architecture for effectively trapping microbial cells.<sup>25</sup> However, these microfilter devices have some limitations, such as clogging of the pores and difficulty in retrieving or dispensing the trapped sample.

Various other methods have also been proposed including  $\mu$ Hall Chip,<sup>28</sup> nanomaterial-based methods,<sup>29–31</sup> the herringbone method,<sup>32</sup> and the evaporation method.<sup>33</sup> For instance, Klapperich's group has demonstrated a low-cost, disposable polymer microfluidic sample preconcentration device that

utilizes evaporation.<sup>33</sup> Their sandwiched architecture device is composed of a top layer of PDMS sample solution, a porous PTFE (Teflon™) membrane layer in the middle, and a pressure driven airflow in the bottom layer. Airflow is used to enhance the evaporation of the sample solution and results in the reduction of the overall fluid volume. Combined with surface-enhanced Raman spectroscopy (SERS), this device successfully detected the targeted bacteria. The SERS signal intensity was a 100-fold enhancement of the signal from the unconcentrated sample.

Here, an agarose-based microfluidic concentrator was built for the rapid determination of the POC concentration of bacteria. The agarose-based microfluidic concentrator was fabricated using agarose with a microchannel of a binary tree design.<sup>34</sup> The agarose layer was then assembled with a square filter paper and a glass slide to form the final device. One end of the channel was blocked for cell collection. Due to the capillary effect and the strong permeability of water in agarose gel, cells

loaded in the reservoir port would flow into the microchannels. In consequence, target cells were collected and concentrated at the end of the microchannels. The system did not require an external complex electric system or a precise pressure driven system for liquid flow or gas flow. The capacity of the agarose-based device was demonstrated. Recovery efficiency above 90% was achieved with a million-fold volume reduction from 400  $\mu\text{L}$  to 400 pL. For concentration of  $1 \times 10^3$  cells  $\text{mL}^{-1}$  bacteria, an enrichment of 7 orders of magnitude in cell density was realized with volume reduction from 100  $\mu\text{L}$  to 1.6 pL. The device was also validated with urine and plasma samples. Finally, plasma samples collected from clinical patients were tested, and the detection of infectious *S. aureus* was achieved using the agarose-based concentrator coupled to an immunofluorescence assay. The agarose-based microfluidic concentrator was rapid, inexpensive, and simple to use and, more importantly, had a high efficiency, thus providing a new method for the POC diagnosis of pathogens.

## MATERIALS AND METHODS

**Materials and Reagents.** Chemicals such as agarose,  $\text{K}_2\text{HPO}_4$ ,  $\text{KH}_2\text{PO}_4$ , Tryptone, Yeast extract, NaCl, BSA, and sodium azide were purchased from Sinopharm Chemical Reagent (Shanghai, China). Rabbit Anti-*E. coli* DH-5 Alpha/FITC (bs-2033R-FITC) and Rabbit Anti-*Staphylococcus* Enterotoxin B/FITC (bs-10722R-FITC) were purchased from Beijing Biosynthesis Biotechnology Co., LTD (Beijing, China).

LB media (1% Tryptone, 0.1% Yeast extract, and 1% NaCl) was prepared for cell culture. Rabbit Anti-*E. coli* DH-5 Alpha/FITC (bs-2033R-FITC) and Rabbit Anti-*Staphylococcus* Enterotoxin B/FITC (bs-10722R-FITC) were diluted 100-fold in stock solution (0.01 M phosphate-buffered saline (PBS), 1% BSA, 0.1% sodium azide, pH = 7.4) before use. Water used for all the solutions preparation was purified by the Direct-Q system (Millipore, Bedford, MA, USA) and filtered with 0.45  $\mu\text{m}$  sterilized syringe filters prior to use.

**Agarose Chip Design and Fabrication.** The design of the passive agarose-based microfluidic concentrator is shown in Figure 1A. An array of microchannels and binary tree structure was designed and fabricated using agarose gel. A rapid prototyping method was performed to fabricate the agarose chips as precisely reported.<sup>34</sup> Briefly, a standard soft-lithography technique was used to fabricate the SU-8 1070 molds on a silicon wafer n type <100>. The agarose layer was made of 2% agarose. After being cured at room temperature, the agarose sheet was peeled from the silicon wafer. To assemble a final concentrator, a PDMS sheet was bonded to the glass slide irreversibly, while a folded filter paper and the agarose sheet was adherent to the glass slide reversibly (Figure 1B). One of the channel ends was used as cell inlet, while the other was closed for the collection of target bacteria. The space between PDMS structure and agarose structure was the reservoir port working as the inlet. Folded filter paper was used as the collection ports for liquid absorption.

**Sample Preparation.** Three different microbial cells, *E. coli* DH-5 Alpha, *E. coli* OP50, and *S. aureus* were selected as the model microbes. To prepare the bacteria samples, 100  $\mu\text{L}$  of frozen cultured bacteria suspension was incubated in 15–20 mL of media in a 25 mL flask, shaken at 200 rpm at 36 °C overnight. Before concentration, 1 mL of liquid culture was centrifuged at 10 000 rpm for 1 min. The pellet was resuspended in 100  $\mu\text{L}$  of LB media. This exchange of media ensured removal of impurities and cell debris.

The concentration of original sample of microbial cells was measured using a bacteria hemocytometer. Then, *E. coli* OP50 was adjusted to the desired organism density prior to use.

**Optical Imaging and Image Analysis.** An inverted fluorescence microscope (IX71, Olympus, Japan) attached with a CCD camera (Evolve S12, photometrics, USA) was employed for imaging. A filter cube of U-MWIB2 (460–490 nm band-pass filter, 505 nm dichroic mirror, 510 nm high-pass filter, Olympus, Japan) was used for monitoring the change in fluorescence intensity.

Acquired images were analyzed using Image Pro Plus 6.0 (MediaCybernetics, Silver Spring, MA, USA). The background image was obtained from a blank microfluidic chip. After the background image was subtracted from the sample image, the fluorescence intensity of the target area was measured automatically using Image Pro Plus 6.0.

**Rapid Passive Bacteria Concentration.** A novel passive microfluidic method was used for the concentration and collection of bacteria. First, the bacteria suspension was logarithmically diluted. Diluted sample solution was then pipetted into the inlet of the microchannels. Due to the capillary effect, the sample added in the reservoir port flowed passively into the microchannel (shown in Figure 1C and Video S1 (ac5026623\_si\_002.avi), Supporting Information). The target infectious bacteria were automatically collected and concentrated in the ends of the microchannels (Video S2 (ac5026623\_si\_003.avi), Supporting Information).

The agarose-based microfluidic concentrator could then be reused. After each run, the device was disassembled and rinsed. Before the next use, the absence of residual cells was confirmed using a microscope.

**On-Chip Immunofluorescence Labeling.** Sample bacteria were added to the inlets of the microchannels, followed by 100  $\mu\text{L}$  of rabbit Anti-*E. coli* DH-5 alpha/FITC. After a 30 min incubation, filtered PBS was added to the reservoir port for rinsing and washing. The final rinsing step was performed three times to ensure the removal of residual rabbit Anti-*E. coli* DH-5 alpha/FITC. Control groups, using *S. aureus* as a negative control without antibody, and a negative control without bacterial cells were also tested.

**Device Storage.** The fabricated device was put in a Petri dish together with a wet filter paper. A cling film was used to wrap the Petri dish before the packaged device was stored in a refrigerator at 4 °C. Typically, the agarose-based device can be kept for two months in the refrigerator. All of the materials were sterilized prior to use.

## RESULTS AND DISCUSSION

**Method Validation.** Before the experiments, a theoretical investigation was carried out for understanding the concentration process using the agarose-based microfluidic chip (Supporting Information). The recovery efficiency was examined to validate the capability of the passive agarose-based microfluidic concentrator. Recovery efficiency was defined as the ratio of the fluorescence intensity of bacteria concentrated into a final volume, divided by the initial fluorescence intensity of the initial sample solution. Concentration of bacteria using microchannel arrays was first carried out, exploring the use of the capillary effect and the good water permeability of the agarose (Figure S1, Supporting Information). Results showed good recovery efficiency for samples with initial concentrations ranging from  $1 \times 10^4$  to  $1 \times 10^8$  cells  $\text{mL}^{-1}$ .

To further evaluate the passive agarose-based microfluidic concentrator, a binary tree structure was designed and fabricated on the agarose layer of the device. As shown in Figure 2A, the root channel (one end of binary tree) was used

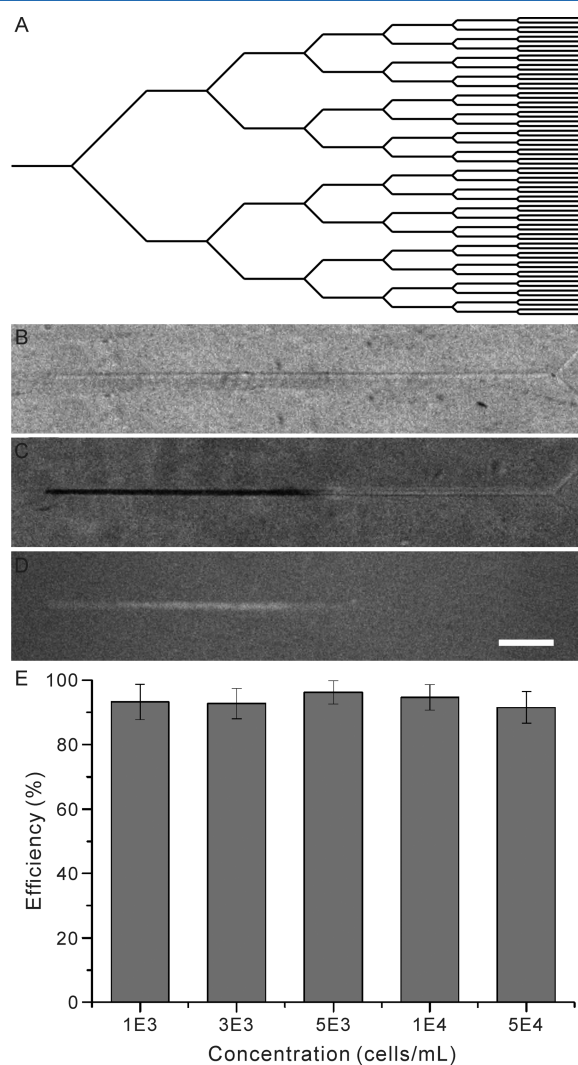


**Figure 2.** (A) Binary tree designs of an agarose-base microfluidic chip. (B) Optical image of the root microchannel. (C) Optical image of cells after bacteria concentration. (D) Fluorescence image of cells after bacteria concentration. (E) Recovery efficiencies using suspensions with different initial concentrations. Scale bar, 200  $\mu\text{m}$ .

for cell concentration, while the leaf channels (64 parallel channels at the other end of the binary tree) were used for cell

loading. Figure 2B shows the details of the terminal of the binary tree chip. The size of each channel was 20  $\mu\text{m}$  (width and height). The concentration of bacteria was performed using the binary tree structure. The collected bacteria are shown in Figure 2C (bright field) and Figure 2D (fluorescence image). The recovery efficiency of the binary tree structure was validated. The results showed that a 400  $\mu\text{L}$  initial volume of bacteria solution at various concentrations ( $5 \times 10^4$ ,  $1 \times 10^4$ ,  $5 \times 10^3$ ,  $3 \times 10^3$ , and  $1 \times 10^3$  cells  $\text{mL}^{-1}$ ) was concentrated into 0.4 nL in the root channel in 30 min with >90% efficiency.

Here, we discussed the reasons for the good performance of the agarose-based microfluidic concentrator. To achieve high recovery efficiency, the whole sample remained in the device due to it having a dead-end design. The main influence on the recovery efficiency was the adsorption and adhesion of bacteria. Agarose is an ideal material for this purpose because it resists the adsorption and adhesion of bacteria.<sup>35,36</sup> An agarose-based device with a dead-end design provided high recovery efficiency. However, one potential disadvantage of this agarose-based device might be the increasing time consumption related to the larger sample volume (shown in Figure S2, Supporting Information). The enrichment of a 100  $\mu\text{L}$  sample could be completed in less than 5 min. Meanwhile, the enrichment of a 500  $\mu\text{L}$  sample might take approximately 20 min. For cell concentration, a continuous capillary force-driven flow ensured the continuous concentration of bacteria in the sample. The use of water-absorbent material at the collection port in the end of the agarose-based chip was very important. Compared to microfilter methods, this agarose-based method did not suffer from clogging. Clogging in microfilter devices significantly increases the hydrodynamic resistance, which reduces flow rates and requires a large pressure. In this agarose-based device, clogging did not prevent the concentration of bacteria for two reasons: the agarose channel walls work as microfilters, and the driving action is provided by capillary force. In conclusion, the dead-end design, the use of agarose-based materials that resist the adsorption of bacteria, and the nonstop concentration process contributes to the good performance.

**$10^7$ -Fold Concentration of Bacteria.** Since infected blood may contain as low as 1–10 CFU  $\text{mL}^{-1}$  of microbial pathogen,<sup>37–41</sup> the detection of low abundant pathogens is a challenging task. Here, the efficiency of low concentration sample enrichment was tested by counting the bacteria collected at the ends of the microchannels. Logarithmic diluted bacteria suspensions ( $10^3$ ,  $10^5$ , and  $10^7$  cells  $\text{mL}^{-1}$ ) were used as sample solutions. The concentration procedure was performed as described above. After concentration, cells in the terminals of the channels were counted. The final cell

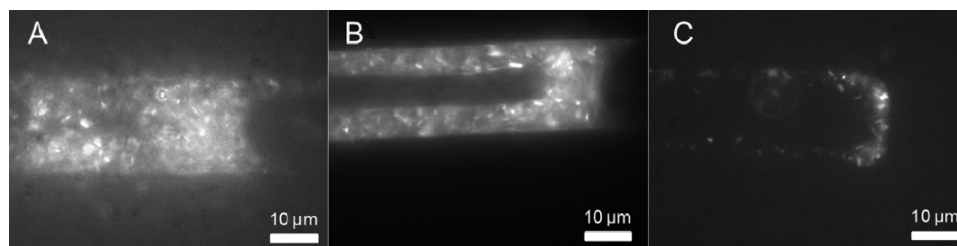


**Figure 3.** Fluorescence images of bacteria after concentration in the end of the microchannels. (A) Results of bacteria suspension with initial concentration of  $10^7$  cells  $\text{mL}^{-1}$ . (B) Results of bacteria suspension with initial concentration of  $10^5$  cells  $\text{mL}^{-1}$ . (C) Results of bacteria suspension with initial concentration of  $10^3$  cells  $\text{mL}^{-1}$ .

density was calculated as the number of cells divided by the volume in the terminals of the microchannels. The bacteria collected are shown in Figure 3. Figure 3A presents the results for an initial concentration of  $10^7$  cells  $\text{mL}^{-1}$  and shows that the ends of the microchannels were full of OPS0. Figure 3B displays the results for an initial concentration of  $10^5$  cells  $\text{mL}^{-1}$ . A large amount of OPS0 was collected and enriched at the end of the microchannels, but the channel was not full. Figure 3C shows the result for an initial concentration of  $10^3$  cells  $\text{mL}^{-1}$ . Only a few bacteria were collected at the end of the channel. The OPS0 bacteria collected at the end of the microchannels were counted. About 20 *E. coli* OPS0 were trapped in the terminal, which were  $4 \mu\text{m}$  in length and  $20 \mu\text{m}$  in both width and height. The final cell density was calculated to be approximately  $10^{10}$  cells  $\text{mL}^{-1}$ . To summarize, results showed that a  $10^7$ -fold concentration was rapidly achieved using the agarose-based microfluidic concentrator. This experiment was finished in less than 10 min. To validate its reproducibility, the experiments were repeated three times using three different devices.

**Dynamics of the Concentration of Bacteria.** The dynamics of the concentration of bacteria were validated using three different initial concentrations. The results are shown in Figure 4. Bacteria concentration experiments were performed using three samples with different initial concentrations ( $8 \times 10^5$ ,  $8 \times 10^4$ , and  $8 \times 10^3$  cells  $\text{mL}^{-1}$ ). The intensity of fluorescence was summed over a measurement window specified by the rectangle in Figure 4A. Figure 4A–E presents time sequence images of the *E. coli* OPS0 collected in the agarose microchannel (also shown in Video S3 (ac5026623\_si\_004.avi), Supporting Information). As shown in Figure 4F, the intensity of fluorescence increased in a stable manner over 140 s. The time point 0 s was the point at which the sample solution was added into the inlets of the microchannels. The intensity of fluorescence increased when the target bacteria flowed into the root channel. For the concentration of the sample with the highest initial cell density ( $8 \times 10^5$  cell  $\text{mL}^{-1}$ ), a fluorescence peak was observed at 45 s. At that time, the highlighted rectangular region was filled with collected bacteria. More bacteria were collected in the branch channels. As shown in Figure 4F, a decrease in the intensity of fluorescence occurred following the peak point. The reasons for this might include the dispersion of bacteria in the collection region and fluorescence bleaching. For initial concentrations of  $8 \times 10^4$  and  $8 \times 10^3$  cells  $\text{mL}^{-1}$ , the intensity of fluorescence increased at a consistent rate in a stable manner. The increasing rate was determined by the initial concentration of bacteria. A higher initial concentration ensured that more bacteria flowed into the root channels within a certain period of time.

**Analysis of Urine and Blood Plasma Samples.** To evaluate the practical applicability of the agarose-based microfluidic concentrator, the system was applied to the concentration of bacteria in urine samples and plasma samples. The plasma was extracted from healthy male volunteers. The extraction time of blank urine from the donor (a healthy male) was about noon before lunch was consumed. Stock standard solutions with bacteria was prepared in PBS buffer and diluted to the final concentration with a blank urine sample and a blank plasma sample. Weak adhesion of the bacteria to the channel walls was observed only in the terminal of the binary tree near the collection region in both the urine samples and the plasma samples. The dynamics of the concentrations of the urine samples and the plasma samples were compared to a standard

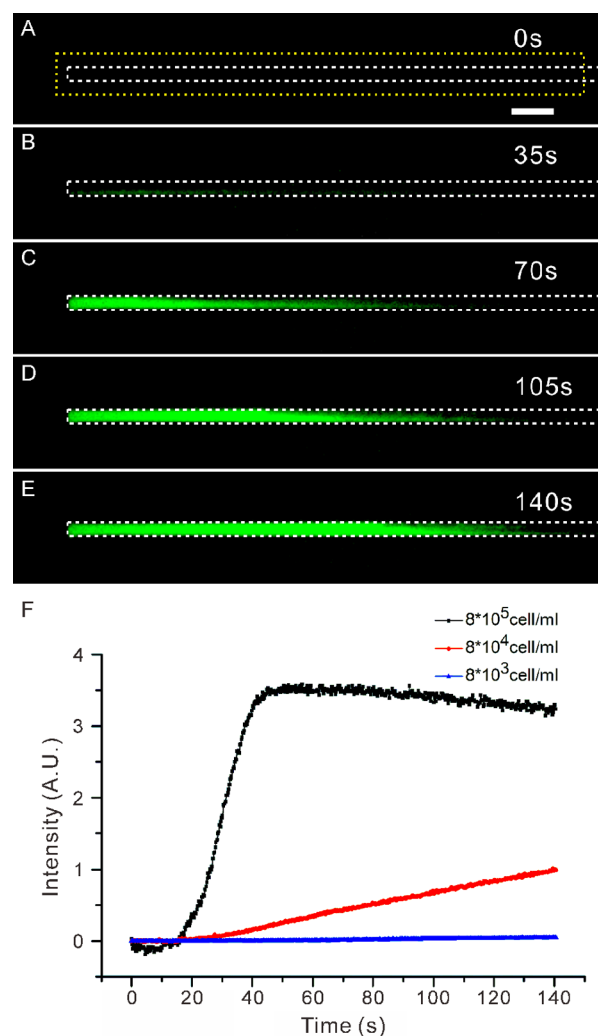


**Figure 4.** Dynamics of bacteria concentration. (A–E) Time sequencing images of automatic bacteria concentration. (F) Dynamics of bacteria concentration using different samples with various initial concentrations. Scale bar,  $60 \mu\text{m}$ .

sample as shown in Figure 5A (initial concentration of  $5 \times 10^5$  cells  $\text{mL}^{-1}$ ). For the urine sample, no significant difference was observed between the standard sample and the urine sample. The concentration of the plasma sample showed a little difference in performance from the standard and the urine samples. First, the concentration of the plasma sample started at  $\sim 43$  s, which was  $\sim 30$  s later than the standard and the urine samples. A steep rise in the fluorescence was only observed for the plasma sample at 43 s. Furthermore, the concentration speed of the plasma sample reached a platform after 100 s, which remained intact for the standard and the urine samples. A possible reason for the above observations might result from the high viscosity of the plasma, leading to slower concentration of bacteria. However, the adhesion of bacteria to the microchannel walls was not significant, thanks to the non-adsorption of agarose to bacteria.

Concentration from the urine samples and the plasma samples of various cell densities was further performed to investigate the performance of the developed method for detecting bacteria in plasma and urine samples. Bacteria suspensions were diluted to 70,  $7 \times 10^2$ ,  $7 \times 10^3$ , and  $7 \times 10^4$  cells  $\text{mL}^{-1}$ . As a result, bacteria with a concentration as low

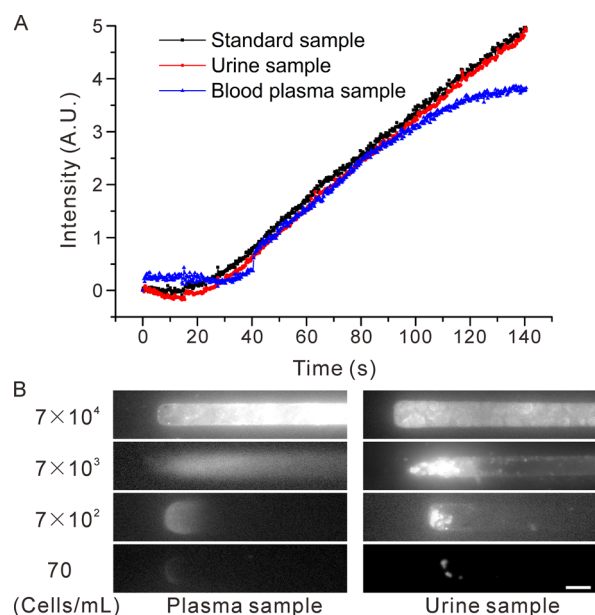


**Figure 5.** (A) Dynamic results using a standard sample, urine sample, and blood plasma sample. (B) Results of concentration using urine samples and blood plasma samples with bacteria of various concentrations. Scale bar, 20  $\mu\text{m}$ .

as 70 cells  $\text{mL}^{-1}$  were detectable in the urine and the plasma samples (shown in Figure 5B). Thus, our results indicated that the agarose-based microfluidic concentrator was suitable for urine samples and plasma samples.

**Clinical Application.** For the analysis of clinical samples, bacteria need to be specifically labeled for optical detection and quantification. Prior to clinical application, detection of pathogens using the fluorescence immunoassay was conducted using standard samples. *E. coli* DH-5 alpha was concentrated in the end of the microchannel, and Anti-*E. coli* DH-5 alpha/FITC was then added into the microchannel to label the cells. After a 10 min rinsing procedure, enriched bacteria were examined under a fluorescence microscope. As shown in Figure S3, Supporting Information, *E. coli* DH-5 alpha was successfully detected. Clinical samples were further tested. Clinical samples were collected from different patients in the Liyuan Hospital, Tongji Medical College, Huazhong University of Science and Technology. Four samples were collected from patients infected with *S. aureus*. Once the blood samples were collected, plasma was separated from the whole blood. For controls, three plasma samples from healthy male donors were obtained. All clinical samples were pre-labeled with Anti-*Staphylococcus* Enterotoxin B/FITC and added to the inlets of the microfluidic chips. After automatic concentration, a PBS buffer was added to remove residual labeling reagents. Figure 6 showed the results for *S. aureus* before (Figure 6C,D) and after (Figure 6A,B) the concentration process. All patient samples gave us positive results using the developed method. The concentration results for the control group are shown in Figure 6E,F without the observation of pathogens, which all gave us negative results. Thus, our detection results were 100% consistent with those obtained from the clinical diagnostics.

Conventional test for pathogen detection involved prolonged culturing of patient samples, which might take 4–7 days to carry out the tests. In contrast, the POC tests using our device could be completed in 30 min. Our method has shown the advantages of reduced analysis time, simplicity to use, labor

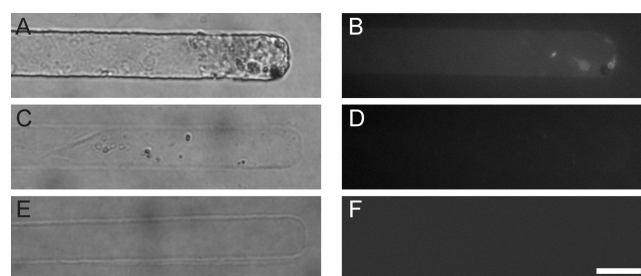


**Figure 6.** POC test with clinical patient sample. (A) Bright field image of concentrated clinical patient sample. (B) Fluorescence image of concentrated clinical patient sample. (C) Bright field image of clinical patient sample before concentration. (D) Fluorescence image of clinical patient sample before concentration. (E) Bright field image of concentrated healthy male sample. (F) Fluorescence image of concentrated healthy male sample. Scale bar, 20  $\mu\text{m}$ .

savings, and low cost, providing a new strategy for POC testing of pathogens.

## CONCLUSIONS

The agarose-based microfluidic chip described in this paper utilizes capillary effects and the permeability of agarose to concentrate microvolume biological samples to pico-volumes in minutes. The fabrication procedure of this device is simple and cheap. It enables the rapid concentration of bacteria at an extremely low cost with high recovery efficiency (above 90%) and good performance. For concentration of  $1 \times 10^3$  cells  $\text{mL}^{-1}$  bacteria, an enrichment of 7 orders of magnitude in cell density was achieved. To further validate the capability of our method to clinical application, detection of *S. aureus* in a patient plasma sample was demonstrated.

Our agarose-based microfluidic method is inexpensive, simple, rapid, and easy to use. The whole agarose-based device did not require an external electric or pressure-driven system. Its simplicity makes it convenient to integrate into other microfluidic systems, including complicated modules such as sample preparation and detection. The agarose-based microfluidic concentrator might represent a powerful novel tool for infectious bacteria detection and point-of-care testing.

## ASSOCIATED CONTENT

### Supporting Information

Information regarding recovery efficiency and detection of DH5 $\alpha$  using the immunology-based method. Figures showing recovery efficiency, concentration time, and immunology-based detection. This material is available free of charge via the Internet at <http://pubs.acs.org>.

## AUTHOR INFORMATION

### Corresponding Author

\*E-mail: [bfliu@mail.hust.edu.cn](mailto:bfliu@mail.hust.edu.cn). Tel: +86-27-87792203. Fax: +86-27-87792170.

### Author Contributions

<sup>†</sup>Y.L. and X.Y. contributed equally to this work.

### Notes

The authors declare no competing financial interest.

## ACKNOWLEDGMENTS

We gratefully acknowledge the financial support from National Natural Science Foundation of China (30970692, 21075045, and 21275060), National Basic Research Program of China

(2011CB910403), and the Innovative Foundation of HUST (2013QN093 and 2013QN090).

## REFERENCES

- (1) Yager, P.; Edwards, T.; Fu, E.; Helton, K.; Nelson, K.; Tam, M. R.; Weigl, B. H. *Nature* **2006**, *442*, 412–418.
- (2) Mabey, D.; Peeling, R. W.; Ustianowski, A.; Perkins, M. D. *Nat. Rev. Microbiol.* **2004**, *2*, 231–240.
- (3) Heo, J.; Thomas, K. J.; Seong, G. H.; Crooks, R. M. *Anal. Chem.* **2003**, *75*, 22–26.
- (4) Mairhofer, J.; Roppert, K.; Ertl, P. *Sensors (Basel)* **2009**, *9*, 4804–4823.
- (5) Giljohann, D. A.; Mirkin, C. A. *Nature* **2009**, *462*, 461–464.
- (6) Mao, X. L.; Huang, T. J. *Lab Chip* **2012**, *12*, 1412–1416.
- (7) Martinez, A. W.; Phillips, S. T.; Whitesides, G. M.; Carrilho, E. *Anal. Chem.* **2010**, *82*, 3–10.
- (8) Beyor, N.; Seo, T. S.; Liu, P.; Mathies, R. A. *Biomed. Microdevices* **2008**, *10*, 909–917.
- (9) Qiu, J. M.; Zhou, Y.; Chen, H.; Lin, J. M. *Talanta* **2009**, *79*, 787–795.
- (10) Buszewski, B.; Szumski, M.; Klodzinska, E.; Dahm, H. *J. Sep. Sci.* **2003**, *26*, 1045–1049.
- (11) Cabrera, C. R.; Yager, P. *Electrophoresis* **2001**, *22*, 355–362.
- (12) Grodzinski, P.; Yang, J.; Liu, R. H.; Ward, M. D. *Biomed. Microdevices* **2003**, *5*, 303–310.
- (13) Kim, M.; Kim, T. *Analyst* **2013**, *138*, 6007–6015.
- (14) Lagally, E. T.; Lee, S. H.; Soh, H. T. *Lab Chip* **2005**, *5*, 1053–1058.
- (15) Lapizco-Encinas, B. H.; Davalos, R. V.; Simmons, B. A.; Cummings, E. B.; Fintschenko, Y. *J. Microbiol. Methods* **2005**, *62*, 317–326.
- (16) Park, S.; Zhang, Y.; Wang, T. H.; Yang, S. *Lab Chip* **2011**, *11*, 2893–2900.
- (17) Pfetsch, A.; Welsch, T. *Fresenius' J. Anal. Chem.* **1997**, *359*, 198–201.
- (18) Podszun, S.; Vulto, P.; Heinz, H.; Hakenberg, S.; Hermann, C.; Hankemeier, T.; Urban, G. A. *Lab Chip* **2012**, *12*, 451–457.
- (19) Pommer, M. S.; Zhang, Y. T.; Keerthi, N.; Chen, D.; Thomson, J. A.; Meinhart, C. D.; Soh, H. T. *Electrophoresis* **2008**, *29*, 1213–1218.
- (20) Puchberger-Enengl, D.; Podszun, S.; Heinz, H.; Hermann, C.; Vulto, P.; Urban, G. A. *Biomicrofluidics* **2011**, *5*, DOI: 10.1063/1.3664691.
- (21) Vykoukal, J.; Vykoukal, D. M.; Freyberg, S.; Alt, E. U.; Gascoyne, P. R. C. *Lab Chip* **2008**, *8*, 1386–1393.
- (22) Balasubramanian, A. K.; Soni, K. A.; Beskok, A.; Pillai, S. D. *Lab Chip* **2007**, *7*, 1315–1321.
- (23) Guo, P.; Hall, E. W.; Schirhagl, R.; Mukaibo, H.; Martin, C. R.; Zare, R. N. *Lab Chip* **2012**, *12*, 558–561.
- (24) Kim, M. C.; Isenberg, B. C.; Sutin, J.; Meller, A.; Wong, J. Y.; Klapperich, C. M. *Lab Chip* **2011**, *11*, 1089–1095.
- (25) Lay, C.; Teo, C. Y.; Zhu, L.; Peh, X. L.; Ji, H. M.; Chew, B. R.; Murthy, R.; Feng, H. H.; Liu, W. T. *Lab Chip* **2008**, *8*, 830–833.
- (26) Perroud, T. D.; Meagher, R. J.; Kanouff, M. P.; Renzi, R. F.; Wu, M. Y.; Singh, A. K.; Patel, K. D. *Lab Chip* **2009**, *9*, 507–515.
- (27) Zhu, L.; Zhang, Q.; Feng, H. H.; Ang, S.; Chauc, F. S.; Liu, W. T. *Lab Chip* **2004**, *4*, 337–341.
- (28) Issadore, D.; Chung, H. J.; Chung, J.; Budin, G.; Weissleder, R.; Lee, H. *Adv. Healthcare Mater.* **2013**, *2*, 1224–1228.
- (29) Kell, A. J.; Stewart, G.; Ryan, S.; Peytavi, R.; Boissinot, M.; Huletsky, A.; Bergeron, M. G.; Simard, B. *ACS Nano* **2008**, *2*, 1777–1788.
- (30) Zhang, L.; Xu, J. J.; Mi, L.; Gong, H.; Jiang, S. Y.; Yu, Q. M. *Biosens. Bioelectron.* **2012**, *31*, 130–136.
- (31) Zhou, R. H.; Wang, P.; Chang, H. C. *Electrophoresis* **2006**, *27*, 1376–1385.
- (32) Jing, W.; Zhao, W.; Liu, S.; Li, L.; Tsai, C. T.; Fan, X.; Wu, W.; Li, J.; Yang, X.; Sui, G. *Anal. Chem.* **2013**, *85*, 5255–5262.
- (33) Zhang, J. Y.; Do, J.; Premasiri, W. R.; Ziegler, L. D.; Klapperich, C. M. *Lab Chip* **2010**, *10*, 3265–3270.
- (34) Li, Y. W.; Feng, X. J.; Du, W.; Li, Y.; Liu, B. F. *Anal. Chem.* **2013**, *85*, 4066–4073.
- (35) Chapman, R. G.; Ostuni, E.; Liang, M. N.; Meluleni, G.; Kim, E.; Yan, L.; Pier, G.; Warren, H. S.; Whitesides, G. M. *Langmuir* **2001**, *17*, 1225–1233.
- (36) Toepke, M. W.; Beebe, D. J. *Lab Chip* **2006**, *6*, 1484–1486.
- (37) Cohen, J. *Nature* **2002**, *420*, 885–891.
- (38) Noursadeghi, M.; Cohen, J. J. R. *Coll. Physicians London* **2000**, *34*, 432–436.
- (39) Opal, S. M.; Girard, T. D.; Ely, E. W. *Clin. Infect. Dis.* **2005**, *41* (Suppl 7), S504–S512.
- (40) Walsh, A. L.; Smith, M. D.; Wuthiekanun, V.; Suputtamongkol, Y.; Chaowagul, W.; Dance, D. A.; Angus, B.; White, N. J. *Clin. Infect. Dis.* **1995**, *21*, 1498–1500.
- (41) Weber, G. F.; Swirski, F. K. *Langenbecks Arch. Surg.* **2014**, *399*, 1–9.